Rodilla Sala, E., Kratzin, H. D., Pick, A. I., & Hilschmann, N. (1991) in *Amyloid and Amyloidosis 1990* (Natvig, J. B., Forre, O., Husby, G., Husebekk, A., Skogen, B., Sletten, K., & Westermark, P., Eds.) pp 161-164, Kluwer Academic Publishers, Dordrecht, Boston, London.
Salinowich, O., & Montelaro, R. C. (1986) *Anal. Biochem. 156*, 341-347.
Saraiva, M. J. M., Birken, S., Costa, P. P., & Goodman, D. S. (1984) *J. Clin. Invest. 74*, 104-119.
Sletten, K., Natvig, J. B., Husby, G., & Juul, J. (1981) *Biochem. J. 195*, 561-572.
Sletten, K., Westermark, P., Pitkänen, P., Thyresson, N., & Olstad, O. K. (1983) *Scand. J. Immunol. 18*, 557-560.
Solomon, A., Frangione, B., & Franklin, E. C. (1982) *J. Clin. Invest. 70*, 453-460.
Solomon, A., Kyle, R. A., & Frangione, B. (1986) in *Amyloidosis* (Glenner, G. G., Osserman, E. F., Benditt, E. P., Calkins, E., Cohen, A. S., & Zucker-Franklin, D., Eds.) pp 449-462, Plenum Press, New York.
Sox, H. C., Jr., & Hood, L. (1970) *Proc. Natl. Acad. Sci. U.S.A. 66*, 975-982.
Tawara, S., Nakazato, M., Kangawa, K., Matsuo, H., & Araki, S. (1983) *Biochem. Biophys. Res. Commun. 116*, 880-888.
Terry, W. D., Page, D. L., Kimura, S., Isobe, T., Osserman, E. F., & Glenner, G. G. (1973) *J. Clin. Invest. 52*, 1276-1281.
Toft, K. G., Setten, K., & Husby, G. (1985) *Biol. Chem. Hoppe*-Seyler *366*, 617-625.
Tonoike, H., Kametani, F., Hoshi, A., Shinoda, T., & Isobe, T. (1985) *Biochem. Biophys. Res. Commun. 126*, 1228-1234.
Tveteraas, T., Sletten, K., & Westermark, P. (1985) *Biochem. J. 232*, 183-190.
Van Camp, B. G. K., Shuit, H. R. E., Hijmans, W., & Radl, J. (1978) *Clin. Immunol. Immunopathol. 9*, 111-119.

Mutations Affecting the Activity of the Shiga-like Toxin I A-Chain†

Robert L. Deresiewicz,‡,§,‖ Stephen B. Calderwood,‡,⊥ Jon D. Robertus,▽ and R. John Collier*,‡

Department of Microbiology and Molecular Genetics, Harvard Medical School, and the Shipley Institute of Medicine, 200 Longwood Avenue, Boston, Massachusetts 02115, Division of Infectious Diseases, Brigham and Women's Hospital, Boston, Massachusetts 02115, Infectious Disease Unit, Massachusetts General Hospital, Boston, Massachusetts 02114, and Department of Chemistry, University of Texas, Austin, Texas 78712

Received July 19, 1991; Revised Manuscript Received December 19, 1991

ABSTRACT: Like ricin, *Escherichia coli* Shiga-like toxin I (SLT-I) inactivates eukaryotic ribosomes by catalytically depurinating adenosine 4324 in 28S rRNA. Although the primary structure of the enzymatic portion of the molecule (Slt-IA) is known to contain regions of significant homology to the ricin A chain (RTA), and although certain residues have been implicated in catalysis, the crystal structure of Slt-IA has not been solved nor has the geometry of its active site been well defined. In order to derive a more complete understanding of the nature of the Slt-IA active site, we placed the *slt*-IA gene under control of an inducible promoter in *Saccharomyces cerevisiae*. Induction of the cloned element was lethal to the host. This lethality was the basis for selection of an attenuated mutant of Slt-IA changed at tyrosine 77, a locus not previously linked to the active site. As well, it permitted evaluation of the toxicity of a number of mutant Slt-IA cassettes that we constructed in vitro. Putative active-site residues implicated in this fashion and in other studies were mapped to an energy-minimized computer model of Slt-IA that had been generated on the basis of the known crystal structure of RTA. A cleft was identified on one face of the protein in which all implicated residues clustered, irrespective of their distances from one another in the primary structure of the molecule. Many of the chemical features anticipated in the active site of an RNA N-glycosidase are indeed present on the amino acid side chains occupying the cleft.

Certain strains of *Escherichia coli* produce Shiga-like toxins (SLTs),[1] potent enterotoxins that have been linked to outbreaks of hemorrhagic colitis, hemolytic uremic syndrome, and thrombotic thrombocytopenic purpura (Dickie et al., 1989; Griffin et al., 1988; Karmali et al., 1985). So named because of their similarity to the classic Shiga toxin (ST) of *Shigella dysenteriae*, the SLTs have been divided into two general groups: SLT-I, which is virtually identical to ST both structurally and immunologically, and SLT-II and its variants, which at the amino acid level are about 60% conserved relative to ST but are not immunologically cross-reactive (O'Brien & Holmes, 1987). All are single-site RNA N-glycosidases that depurinate a specific adenosine of 28S eukaryotic rRNA (A_{4324} in rat ribosomes) and thereby irreversibly inhibit protein synthesis (Endo et al., 1988), a phenomenon that results in the death of the target cell.

SLT-I has a molecular mass of ~70 kDa and is composed of a single A subunit (Slt-IA; 32.2 kDa) and multiple copies

† This work was supported by Grants AI22021 and AI22848 (to R. J.C.) and AI27329 (to S.B.C.) from the National Institute of Allergy and Infectious Diseases, by the Infectious Diseases and Basic Microbiological Mechanisms Institutional Training Grant NIH ADAMHA T32AI07061-13 and the National Foundation for Infectious Diseases–Squibb Clinical Fellowship in Gram-Negative Infections (to R.L.D.), and by Grant GM30048 from the National Institutes of Health (to J.D.R.).

* Corresponding author.
‡ Harvard Medical School and the Shipley Institute of Medicine.
§ Brigham and Women's Hospital.
‖ Present address: Channing Laboratory, Department of Medicine, Brigham and Women's Hospital, 180 Longwood Ave., Boston, MA 02115.
⊥ Massachusetts General Hospital.
▽ University of Texas.

[1] Abbreviations: SLT-I, Shiga-like toxin I holotoxin; Slt-IA, Shiga-like toxin IA subunit; *slt*-IA, Shiga-like toxin IA gene; ST-A, Shiga toxin A subunit; RTA, ricin A chain; PCR, polymerase chain reaction; CFU, colony-forming units; CRM, cross-reactive material.

0006-2960/92/0431-3272$03.00/0

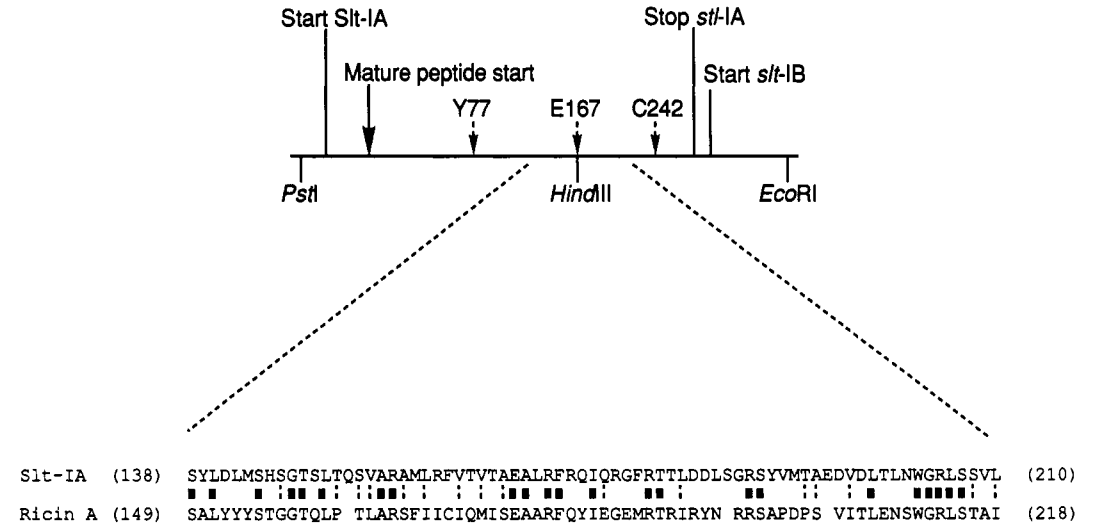

FIGURE 1: Map of *slt*-IA as it appears in pSC25. The entire *slt*-IA coding sequence and the proximal one-third of the *slt*-IB coding are cloned between the *Pst*I and *Eco*RI sites in the pUC19 polylinker. The region of highest homology between the Slt-IA chain and the ricin A chain is highlighted. Identical residues are indicated with a closed box. Chemically similar residues are indicated with a dashed line. Adapted from Calderwood et al. (1987).

of a noncovalently linked B subunit (Slt-IB; about 7.5 kDa). The B subunit complex functions in target cell receptor recognition, while the A subunit is catalytically active. Reduction of a single intrachain disulfide bond and mild proteolysis of the A subunit give rise to two smaller pieces: A_1 (~27.5 kDa), which constitutes the N-terminal portion of the molecule, and A_2 (~3–4 kDa), which constitutes the C-terminal portion. The A_1 fragment is reported to be at least 6 times more active in protein synthesis inhibition than is the whole A subunit (Olsnes et al., 1981; Reisbig et al., 1981).

The *slt*-IA gene has been cloned and sequenced (Calderwood et al., 1987). The primary structure of its deduced daughter protein is highly homologous to the catalytic domain of the plant toxin ricin (ricin A chain; RTA), itself the prototype of an emerging family of structurally related RNA-binding proteins that includes cytotoxins such as abrin and modeccin and ribosome-inhibiting proteins such as trichosanthin and pokeweed antiviral protein. Like the SLTs, all are single-site RNA N-glycosidases (Endo et al., 1987; Endo & Tsurugi, 1987). The crystal structure of ricin has been solved to 2.5-Å resolution and is notable for the presence of a prominent cleft on one face of the protein, believed to be the active site (Katzin et al., 1991; Montfort et al., 1987). Regions of SLT with greatest similarity to ricin map to that cleft, which in the primary structure of ricin falls between residues 149 and 218 (138 and 210 in SLT-IA; Figure 1) (Calderwood et al., 1987). Much experimental work has focused on the most highly conserved portions of that cleft. In separate studies, the conservative change E167D was shown to diminish by 2–3 orders of magnitude the activity of both Slt-IA and Slt-IIA (Hovde et al., 1988; Jackson et al., 1990). The corresponding change E177D attenuated the activity of the ricin A chain by about 80-fold (Schlossman et al., 1989), and the nearby change R180H abolished enzymatic activity altogether (Frankel et al., 1990). In Slt-IIA, the combined substitution and deletion mutation L201V + Δ202–213 eliminated vero-cell cytotoxicity of the assembled holotoxin (Jackson et al., 1990).

Until now all recombinant genetic work on Shiga toxin/SLT has been done in prokaryotes, the ribosomes of which are insensitive to the toxins' effects. Accordingly, mutations at putative key residues had to be created in vitro and their functional effects assessed in vitro. Obviously such a strategy is biased by the investigator's conception of the active site: one chooses to alter those residues that one believes are likely involved in catalysis. Perhaps a more powerful technique is one that permits direct selection of spontaneously-arising attenuated mutant protein products. Mutations selected in that way, provided that they are not truncated and that they fold normally, are likely at residues critical for catalysis, because it was the loss of catalytic function caused by those mutations that led to their selection in the first place.

Frankel and colleagues have recently pioneered such a system for selection of point mutants of RTA in *Saccharomyces cerevisiae*, a eukaryote whose ribosomes are sensitive to its action (Frankel et al., 1989). Intracellular expression of wild-type RTA was lethal to the yeast host cells. Plasmids encoding mutant RTA were therefore readily identified by their failure to kill *S. cerevisiae*. In this manner, several functionally relevant point mutations in the ricin coding sequence were selected.

Here we report our experience with an analogous system that we established to study the active site of Slt-IA. *slt*-IA was placed under control of an inducible promoter in *S. cerevisiae*. Induction of the cloned element was lethal to the host. This lethality was the basis for selection of an attenuated mutant of Slt-IA changed at residue 77, a locus known to be conserved in the ricin family but not previously studied in Slt-IA. An attractive ancillary benefit of our system was the ability it gave us to test the activity of several well-defined deletion mutations that we constructed in vitro. We were thus able to screen several hundred randomly arising yeast survivors as well as 16 defined deletion cassettes and to select for further study only those species with interesting properties. By correlating structural data derived in this way with a computer-generated, energy-minimized model of Slt-IA, we were able to gain new insight into the geometry of the Slt-IA active site.

Materials and Methods

Plasmids and Strains. pSC25, which contains the intact *slt*-IA gene and a truncated portion of *slt*-IB under control of the *lacZ* promoter in pUC19, was available to us from previous studies. So too was pSC25.1, a derivative of pSC25 containing a single-base mutation that effects the amino acid change E167D in SLT-IA. pRY131, a 2μ-based multicopy yeast expression plasmid, was kindly provided by Arthur

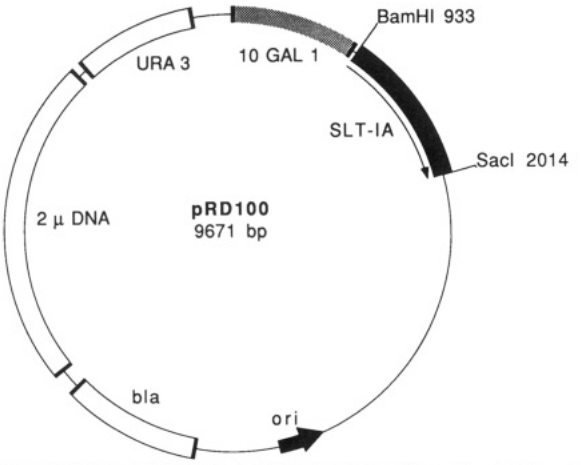

FIGURE 2: Map of pRD100. pRD100 contains the entire *slt*-IA coding sequence and the proximal one-third of the *slt*-IB coding sequence on a *Bam*HI–*Sac*I cassette that was constructed by PCR. The cassette was cloned between the *Bam*HI and *Sst*I sites of pRY131, just downstream of the inducible *Gal1-10* promoter. Also shown are *ura*3 and the 2μ control element for selection and maintenance in *S. cerevisiae* and *bla* and *ori* for selection and maintenance in *E. coli*. pRD100(E167D) is identical, save for the point mutations described in the text.

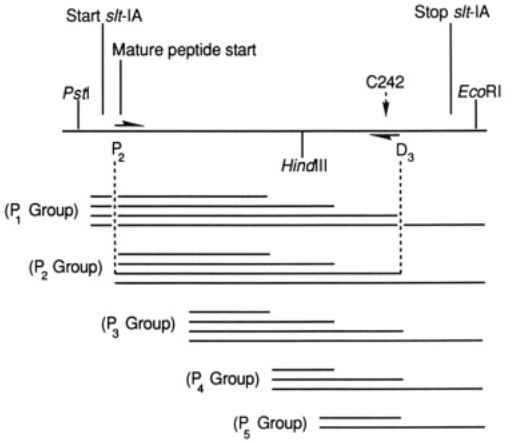

FIGURE 3: Nested deletions made by PCR: This schematic diagram illustrates 17 derivative cassettes that were constructed from *slt*-IA by the polymerase chain reaction. In the upper part of the figure in the map of *slt*-IA as it appears in pSC25. Below are 17 horizontal lines, each representing a single cassette and each spanning that region of *slt*-IA that is contained in the cassette. The cassettes are defined by the identities of the proximal and distal oligonucleotide primers which were used to create them. For example, cassette P_2–D_3, the shortest of the cassettes that retained toxicity (highlighted by vertical dashed lines), was created by pairing proximal primer P_2 (rightward-pointing arrow) with distal primer D_3 (leftward-pointing arrow). Four cassettes begin with primer P_1, which is located at the native ATG start site (depicted by the uppermost group of four horizontal lines). Within that group is a cassette that ends at distal primer D_1 (i.e., at N131, designated cassette P_1–D_1), one that ends at distal primer D_2 (i.e., at G187; P_1–D_2), one that ends at distal primer D_3 (i.e., at G255; P_1–D_3), and one that ends at distal primer D_4 (i.e., beyond the end of the native *slt*-IA coding sequence; P_1–D_4). The other cassettes were constructed in an analogous fashion. The precise locations of primers P_2–P_5 are as follows: P_2, mature start; P_3, codon N65; P_4, codon H133; and P_5, codon L201. In a circumstance where a proximal primer would be downstream of a distal primer (such as a pairing of P_5 with D_1), a productive PCR cannot occur. Accordingly, the P_4 and P_5 groups have fewer than four members.

Frankel (Department of Medicine, Duke University, Durham, NC). It contains the *URA3* gene and the *GAL1-10* promoter for selection and expression in yeast, as well as the pBR322 *ori* and *bla* for selection and propagation in *E. coli*. DNA cloning, single-stranded DNA production, and periplasmic toxin expression were carried out in the *E. coli* K-12 strain TG1 [Δ(*lac–pro*) *supE thi hsdD5*/F′ *traD36 proA*$^+$*B*$^+$ *lacI*^{q} *lacZ* ΔM15] or GM-1 [Δ(*lac–pro*) *thi*$^-$/F′ *lacI*^{q} *lacPL8 pro*$^+$]. Yeast plasmids were recovered into *E. coli* strain DH5α [F$^-$ ϕ80d*lacZ*ΔM15 Δ(*lacZYA–argF*)U169 *deoR recA1 endA1 hsdR17* (r_K^-, m_k^+) *supE44* λ^- *thi-1 gyrA96 relA1*]. All yeast experiments were performed in *S. cerevisiae* strain Fy2 [mating type α, *ura3-52*], the gift of Fred Winston (Harvard Medical School, Boston, MA).

Oligonucleotides. All oligonucleotides used in this study were synthesized on an Applied Biosystems Model 381A DNA synthesizer and purified with use of the manufacturer's oligonucleotide purification cartridges.

Construction of Yeast Expression Vectors Encoding Slt-IA. The polymerase chain reaction (PCR) was used to create *Bam*HI–*Sac*I cloning cassettes as follows: Oligonucleotide primers 5′-CCAGGATCCGGAGTATTGTGTAATATG-3′ and 5′-GAATTCGAGCTCGGT-3′ were prepared. The first oligonucleotide (designated P_1) contains a three-base leader, a *Bam*HI site (underlined), and the 18 bases immediately upstream of and including the ATG start site of *slt*-IA in pSC25. The second oligonucleotide (designated D_4) is complementary to a portion of the pUC19 polylinker distal to the *slt* insertion site in pSC25. An internal *Sac*I site is underlined. Ten cycles of amplification (denature 95 °C, 1 min; anneal 55 °C, 1 min; polymerize 72 °C, 3 min) were carried out with a Perkin-Elmer–Cetus thermal cycler and the manufacturer's GeneAmp kit as recommended, beginning with 1 ng of pSC25 or pSC25.1 template DNA and 100 nmol of each primer. The resultant *slt* cassettes were serially digested with *Sac*I and *Bam*HI and recovered in M13mp18. PCR fidelity was verified by complete sequencing of the *slt*-IA portion of each, as previously described. The cassettes were then excised and subcloned between the *Bam*HI and *Sst*I sites of pRY131 to create the plasmids pRD100 (Figure 2) and pRD100(E167D), respectively.

A similar strategy was used to produce a series of cassettes bearing defined nested deletions of the *slt*-IA gene: Seven additional primers were synthesized. Four contain sequences *identical* to oligonucleotide regions of the *slt*-IA gene ("proximal primers", designated P_2 through P_5), while three contain sequences *complementary* to regions of the *slt*-IA gene ("distal primers", designated D_1 through D_3). The proximal primers all begin with the sequence 5′-CCAGGATC-CATG..., while the distal primers all begin with the sequence 5′-TTCGAGCTCA.... *Bam*HI and *Sac*I sites are again underlined. As illustrated in Figure 3, the primers are distributed fairly evenly along the linear structure of the gene in the forward and reverse directions. The precise alignment of the distal primers was chosen so that the stop codons (complement of 5′...TCA...) would be in the *slt*-IA reading frame. PCR was carried out with all combinations of proximal and distal primers and resulted in 16 cassettes truncated at either the 5′ end, the 3′ end, or both. Cassettes so obtained (designated P_i–D_j) were ligated into pRY131 as described above.

Yeast Transformation, Maintenance, and Plasmid Recovery. Yeast cells were transformed by the lithium chloride method (Sherman et al., 1986). Transformants were selected on synthetic complete medium lacking uracil and containing 2% glucose. Strains were maintained as glycerol stocks at −70 °C. Plasmids were recovered from yeast for analysis with a modification of the smash-and-grab procedure (Hoffman & Winston, 1987): yeast cells were grown up overnight at 30 °C in 5 mL of selective broth containing 2% glucose and sequentially pelleted in a microcentrifuge. The cell pellets were

resuspended in 200 μL of buffer (1% SDS, 2% Triton X-100, 100 mM NaCl, 10 mM Tris, pH 8.0, and 1 mM EDTA); 200 μL of phenol–chloroform (Maniatis et al., 1982) and 0.3 g of acid-washed glass beads were added and the mixture was agitated at maximum power in a desktop vortex mixer for 2 min. The crude lysate was spun for 5 min and the aqueous phase harvested into an equal volume of TE (10 mM Tris, pH 7.5, and 1 mM EDTA). The resultant mixture was extracted once each with phenol, phenol–chloroform, and chloroform and either used for electroporation directly or ethanol-precipitated first. One microliter was used to transform 40 μL of electrocomponent *E. coli* DH5α using the Gene Pulser electroporation apparatus (Bio-Rad Laboratories, Richmond, CA) according to the manufacturer's instructions: electrode gap 0.2 cm, electrical field 12.5 kV/cm, capacitor 25 μF, pulse controller 200 Ω, expected time constant 4.5–5 ms.

Growth Properties of Transformed Yeast Cells. For solid-phase growth experiments, single colonies of transformed yeast cells were streaked in duplicate onto uracil-deficient synthetic medium supplemented with either 2% glucose or 2% galactose. Growth was monitored for 72 h and scored as positive or negative.

For measurement of growth kinetics in broth cultures, individual strains were grown up overnight in 5 mL of selective broth containing 2% glucose. The next day an aliquot of each was diluted in the same medium to an OD_{540} of ~0.100 (which corresponds to a cell density of about 1×10^6 CFU/mL) in a total volume of 60 mL in a 250-mL baffled shake flask. The cultures were incubated at 30 °C and 250 rpm. When the cells had reentered log-phase growth, they were centrifuged, washed once with cold water, split, and resuspended in 30 mL of selective broth containing either 2% glucose or 2% galactose. Incubation was continued in parallel in 125-mL baffled shake flasks. Aliquots were periodically withdrawn for measurement of OD_{540} and colony-forming units per milliliter. The number of colony-forming units per milliliter was determined by plating 200 μL of 10-fold serial dilutions of the broths in 3 mL of uracil-deficient/2% glucose top agar (0.75% Bacto-agar) on uracil-deficient/2% glucose plates. Each measurement was performed in duplicate. Colonies were counted at 72 h, and the number of colony-forming units per milliliter of the original culture was calculated.

Selection of Mutant slt-IA Genes. Yeast cells bearing pRD100 (wild-type *slt-IA*) were grown up overnight in selective broth containing 2% glucose. The next day they were diluted in the same medium to a concentration of ~2–5 CFU/mL. Aliquots (200 μL) were distributed to each well of several 96-well microtiter dishes, which were incubated for 2 days at 30 °C. The contents of each turbid well was recovered separately, rinsed with water, and plated in toto on uracil-deficient/galactose plates. Colonies growing on the galactose plates at 72 h were streak-purified on the same medium; single colonies were used for further studies.

To assess whether candidate mutant clones produced immunoreactive protein, strains were grown to early log phase in uracil-deficient medium containing 2% raffinose (a noninducing, nonrepressing sugar relative to the *GAL1* promoter). Transcription was induced by the addition of 0.1 volume of 20% galactose, and the cells were incubated for an additional 6–8 h. Induced cells were collected by centrifugation and solubilized in SDS sample buffer (15 mM Tris, pH 6.8, 0.8% SDS, and 1.25% β-mercaptoethanol). They were heated for 2 min in boiling water, immediately chilled on ice for 5 min, and then centrifuged for 2 min. The resulting supernatant was referred to as whole-cell yeast extract. The nonparticulate portion was mixed with 0.2 volume of 5× tracking dye (40% glycerol and 0.35% bromophenol blue) and the proteins therein separated by electrophoresis through 11.25% polyacrylamide/sodium dodecyl sulfate gels. Low-range prestained molecular weight standards (Bio-Rad) and purified Shiga toxin (kindly provided by A. Donohue-Rolfe, Tufts University School of Medicine, Boston, MA) were applied to each gel. Electrophoretic transfer of the separated proteins to nitrocellulose was done as previously described (Hovde et al., 1988). Immunoreactive bands were visualized by sequential incubation with polyclonal rabbit anti-Shiga toxin antiserum (kindly provided by A. Donohue-Rolfe) and 1 μCi of ^{125}I-protein A (Amersham Corp, Arlington Heights, IL), followed by autoradiography overnight at −70 °C using Kodak XRP-1 film (Eastman Kodak, Rochester, NY) and one Cronex intensifying screen.

To assess whether the mutant phenotype of CRM-positive yeast cells that were able to grow on galactose was plasmid-borne, the plasmids contained therein were recovered and used to transform naive *S. cerevisiae* cells. Growth characteristics of the resultant transformants were assessed as described above.

Site-Directed Mutagenesis. The 1152-bp *Pst*I–*Eco*RI fragment of pSC25 was ligated into M13mp18 to construct M13mp18.25. Synthetic oligonucleotides were prepared that encoded the discrete single-site amino acid substitutions Y77F or Y77S in *slt*-IA (Y77F, 5′-CGA-AAT-AAT-TTA-TTT-GTG-ACA-GGA-TTT-GTT-3′; Y77S, 5′-CGA-AAT-AAT-TTA-TCT-GTG-ACA-GGA-TTT-GTT-3′). Site-directed mutagenesis of M13mp18.25 was performed with the Amersham oligonucleotide-directed in vitro mutagenesis system according to the manufacturer's protocols. Candidate mutant clones were screened by limited DNA sequencing through the region of the desired point mutation. Fidelity of the mutagenesis reactions was next verified by complete sequencing of positive clones. The altered *Pst*I–*Eco*RI fragments were returned to pUC19 to generate the mutant expression plasmids pRD400 (Y77F) and pRD410 (Y77S).

For other experiments, the PCR-generated *Bam*HI–*Sac*I fragment of pRD100 was ligated into M13mp18 to construct M13mp18.100. Site-directed mutagenesis of that template with the oligonucleotide Y77F was performed exactly as described above, except that the altered fragment was returned to pRY131 to create pRD100(Y77F).

Expression of Wild-Type and Mutant Slt-IA in E. coli. Wild-type or mutant Slt-IA was expressed in strains of TG1 containing pSC25 (wild-type), pSC25.1 (E167D), pRD400 (Y77F), or pRD410 (Y77S). TG1 bearing pUC19 served as the negative control. Strains were maintained on minimal medium/glycerol plates deficient in proline, supplemented with 50 μg/mL ampicillin. This medium exhibits low catabolite repression relative to the *lac* promoter. Overnight cultures were prepared in broth of similar composition, diluted to an OD_{600} of about 0.100 in fresh minimal medium with ampicillin, and grown at 37 °C and 250 rpm to mid-log phase (OD_{600} of about 0.500). Isopropyl β-D-thiogalactopyranoside (IPTG) was added to a final concentration of 1 mM and the incubation continued for an additional 2 h. The cells were chilled on ice for 10 min. Ten to fifteen OD_{600} units of cells were centrifuged at 15000*g* for 5 min at 4 °C. The cell pellets were resuspended in 400–600 μL of phosphate-buffered saline (PBS; 10 mM phosphate buffer and 140 mM NaCl, pH 7.4) containing 2 mg/mL polymyxin B sulfate at 7200 USP units/mg (Sigma Chemical Co., St. Louis, MO), incubated for 10 min at 4 °C, and centrifuged at 15000*g* for 2 min at 4 °C. The supernatant

was harvested directly into 1.5 mL of HEPES buffer (20 mM HEPES, pH 7.4, 15% glycerol, 20 mM DTT, and 100 μg/mL BSA) and spun to the dead volume (about 50 μL) at 4000*g* in a Centricon-10 ultrafiltration device (Amicon, Beverley, MA). An additional 2 mL of HEPES buffer was added and the sample respun as before. The retained material was referred to as periplasmic extract and was used immediately or stored at −20 °C until use. Proteins therein were solubilized in sample buffer and separated through 12.5% polyacrylamide/sodium dodecyl sulfate gels. Immunoreactive products were visualized as described above.

Assay of Protein Synthesis Inhibition. Periplasmic extracts containing wild-type or mutant Slt-IA were analyzed for their capacity to inhibit protein synthesis in a cell-free system with rabbit reticulocyte lysate and brome mosaic virus mRNA as previously described (Hovde et al., 1988). Periplasmic extracts were preincubated with the reticulocyte lysate at 37 °C for 30 min to allow the toxin to act on the ribosomes before the start of the protein synthetic reaction. The degree of incorporation of radiolabel into acid-precipitable material after preincubation of the reticulocyte lysate with HEPES buffer alone was used as the positive control. For the negative control, mRNA was omitted.

Molecular Modeling. The basis for the molecular model of Slt-IA was a refined model of RTA that was used as a three-dimensional template (Katzin et al., 1991). First the amino acid sequence of Slt-IA was aligned with that of RTA to maximize the number of amino acid identities. Next, amino acid substitutions, insertions, and deletions were made to the three-dimensional RTA model on the basis of linear sequence alignment with Slt-IA, using the program FRODO (Jones, 1978) on a PS390 graphics system (Evans and Sutherland, Salt Lake City, UT). Stereochemical clashes that resulted from the amino acid changes were adjusted by hand on the graphic system, maintaining as much of the RTA geometry as possible.

Thereafter, the net number of unfavorable van der Waals contacts in the crude, hand-adjusted model for Slt-IA was further reduced by subjecting it to 40 cycles of energy minimization with the harmonic repulsive term option of XPLOR (Brunger et al., 1987). Finally, iterative cycles of minimization against a Lennard-Jones potential were carried out until the overall incremental energy change for the model on each cycle was less than 10 kJ/mol.

The atom-record file so created was displayed and studied on a Dell 386 personal computer with the Promodeler I software package (New England BioGraphics, Peacham, VT).

Results

Expression of SLT-IA in S. cerevisiae. pRY131, the yeast shuttle vector used in this study, replicates to moderate copy number in *S. cerevisiae*. Its *Bam*HI site is located 39 codons downstream of the native *GAL1* translational start site. Thus, constructs cloned between the *Bam*HI and *Sac*I sites are expressed as fusion proteins with 39 vector-derived amino acids preceding the amino terminus of the cloned protein itself. As indicated in Figure 2, pRD100 and pRD100(E167D) contain the signal sequence and the entire coding sequence of *slt*-IA as well as the proximal one-third of *slt*-IB inserted between the *Bam*HI and *Sac*I sites of pRY131.

Complete sequencing of the PCR-generated *Bam*HI–*Sac*I cassette in pRD100 revealed two base changes presumably introduced by the PCR. Both were T to C transitions in the third position of their respective codons (V98 and R268). Neither altered the implied amino acid sequence of the daughter protein. Sequencing of the corresponding cassette in pRD100(E167D) confirmed the expected change at E167 and revealed no additional mutations.

Table I: Growth of Yeast Strains on Various Sugars[a]

plasmid	growth on glucose	growth on galactose
pRY131	+	+
pRD100	+	−
pRD100(E167D)	+	+
pRD100(Y77S)	+	+
pRD100(Y77F)	+	haze[b]
pRD100(1–3)	+	−
pRD100(2–3)	+	−

[a] Single colonies of transformed yeast cells were streaked in duplicate onto uracil-deficient synthetic medium supplemented with either 2% glucose or 2% galactose. Growth was monitored for 72 h and scored as positive or negative. [b] Refers to an intermediate result that occurred with this plasmid only.

As shown in Table I, yeast transformed with pRD100 grew normally on uracil-deficient plates supplemented with glucose but failed to grow at all on uracil-deficient plates supplemented with galactose. Control yeast transformed with pRY131 grew equally well on either carbon source. The effect was also demonstrable in broth cultures: early log-phase cells resuspended in glucose broth promptly resumed log-phase growth regardless of the plasmid that they carried and saturated at a cell density of $\sim 2 \times 10^8$/mL. Following a lag period during which galactose-inducible genes were activated, the control strain (pRY131) resuspended in galactose broth also eventually reentered log-phase growth and saturated at a similar cell density. The strain carrying pRD100, however, showed a rapid and marked decline in viable cell density on activation of galactose-inducible genes (Figure 4A).

As expected from the known attenuating effect of the E167D mutation on Slt-IA activity, Fy2(pRD100(E167D)) grew equally well on glucose or galactose, both on solid media and in broth culture (Table I, Figure 4B).

Western blot analysis of whole yeast cell extracts with polyclonal anti-Shiga toxin antiserum revealed that Fy2(pRD100) and Fy2(pRD100(E167D)) both made an immunoreactive product corresponding to the size of the expected full-length fusion protein (data now shown). Fy2(pRY131) did not make immunoreactive product.

Plasmids recovered with the yeast strains were transformed into naive *S. cerevisiae* host cells and retested, which analysis verified that the above-described phenotypes were indeed plasmid borne.

Generation of Mutant SLT-IA Cassettes in S. cerevisiae. Randomly arising galactose-resistant derivatives of Fy2(pRD100) were easily obtained as described; ~250 such clones were screened for production of immunoreactive Slt-IA. Eleven positive clones were identified, of which one made full-length protein. The derivative plasmid therein was isolated and returned to naive Fy2 cells. Those, too, made immunoreactive Slt-IA and were able to grow on galactose, a result verifying that the galactose-resistant phenotype was plasmid borne. Sequencing of the *slt*-IA gene in that mutant plasmid revealed a single base change in codon 77 effecting the amino acid substitution Y77S. Broth-culture growth experiments (Figure 4B) confirmed that toxicity of pRD100(Y77S) was attenuated to a degree similar to that of pRD100(E167D).

To test the effect of a more conservative amino acid substitution at locus 77, the mutant pRD100(Y77F) was constructed by site-directed mutagenesis. The phenotype of that mutant was intermediate between those of pRD100 (wild-type SLT-IA) and pRD100(E167D) (Table I and Figure 4B). Western blot confirmed that it produced full-length immunoreactive product.

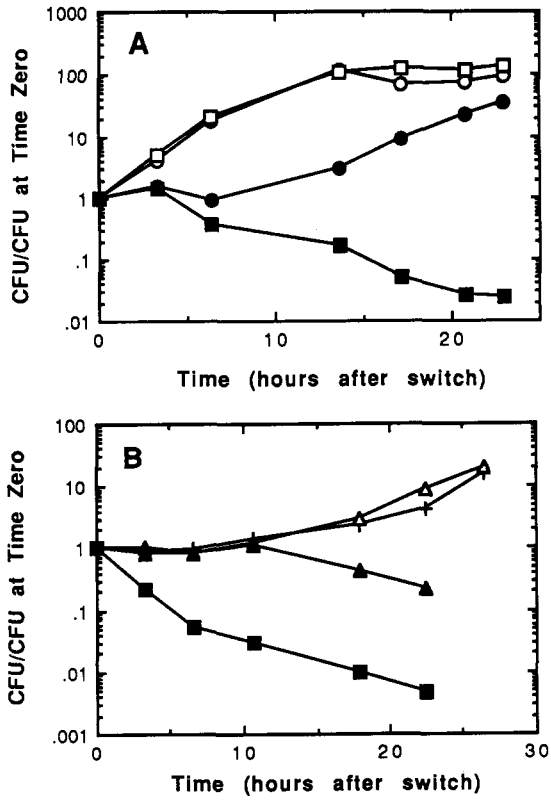

FIGURE 4: (A) Growth in various sugars of yeast cells bearing pRY131 or pRD100. At T_0, early log-phase cultures that had been growing in glucose broth were harvested, washed, and split to either glucose or galactose broth. Incubation was resumed. Data points reflect the number of colony-forming units per milliliter in each culture at time T divided by the number in that same culture at time T_0. pRY131/glucose (○), pRY131/galactose (●), pRD100/glucose (□), pRD100/galactose (■). (B) Growth in galactose broth of yeast cells bearing wild-type or mutant *slt*-IA. These experiments were performed exactly as those in panel A. In this graph, only the galactose arm of the experiment is illustrated. pRD100 (■), E167D (+), Y77S (△), Y77F (▲).

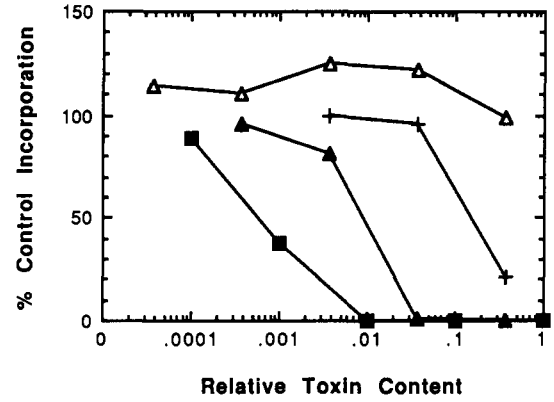

FIGURE 5: Inhibition of protein synthesis by wild-type and mutant periplasmic extract. Aliquots of rabbit reticulocyte lysate were preincubated for 30 min with various dilutions of periplasmic extract containing wild-type or each of the three mutant Slt-IA species. The lysates were then assayed for protein synthesis and compared to control lysates preincubated with extracts derived from pUC19-bearing host cells. Background activity (mRNA omitted) was subtracted from each value. Data were normalized for the minor differences in immunoreactive toxin in each test extract and plotted as a percentage of control protein synthesis as a function of relative toxin content. The assay was performed a minimum of two times on each mutant. Shown are the results of one representative experiment. Wild-type Slt-IA (■), E167D (+), Y77S (△), Y77F (▲).

Expression of Wild-Type and Mutant SLT-IA in E. coli. In order to generate quantitative data regarding the degree of attenuation of the locus 77 mutants, we introduced the corresponding changes into pSC25, the pUC19-based Slt-IA *E. coli* expression plasmid. All constructs were verified by complete DNA sequencing. Periplasmic extract was prepared in parallel from *E. coli* strains bearing pUC19 (negative control), pSC25 (positive control), and each of the mutant strains pRD400(Y77F), pRD410(Y77S), and pSC25.1-(E167D). Extracts of strains carrying mutant plasmids contained between one-quarter and one-half the amount of full-length immunoreactive product contained in extracts produced from the wild-type strain, as judged by Western blots of serial 2-fold dilutions of each, as previously described (Hovde et al., 1988) (data not shown). In addition, each extract, including that of the wild-type strain, contained one major and several minor breakdown products. The amount and the relative distribution of the breakdown products was identical from extract to extract. As expected, the strain containing pUC19 produced no immunoreactive material.

Inhibition of Protein Synthesis by Periplasmic Extract. As shown in Figure 5 and as previously reported (Hovde et al., 1988), extracts containing wild-type Slt-IA were highly active, whereas extracts containing the mutant E167D were markedly attenuated (~220–400 fold in these experiments). The mutant Y77S was completely inactive even at the highest concentration tested and is thus attenuated at least 1000-fold. The mutant Y77F was moderately attenuated, typically showing between 10- and 20-fold less activity than the wild type.

Deletion Analysis. In order to define the smallest possible fragment of Slt-IA that retained toxicity to yeast cells, a total of 17 *slt*-IA cassettes were made with all possible productive combinations of proximal and distal PCR primers (Figure 3). Cassettes *beginning* with primer P_1 start with the signal sequence. In cassettes beginning with primer P_2, the signal sequence is deleted and the cassettes start at the first residue of mature Slt-IA. Those beginning with primers P_3, P_4, and P_5 start at Slt-IA codons 65, 133, and 201, respectively. Cassettes *ending* with primers D_1 and D_2 end, respectively, at codons 137 and 187. Cassettes ending with primer D_3 are truncated at codon 255 and so end at approximately the same amino acid residue as does the A_1 fragment. Cassettes ending with primer D_4 terminate beyond the end of the *slt*-IA coding sequence. Thus, cassette P_1–D_4 encodes full-length Slt-IA protein, including the signal sequence, and is identical to that contained in pRD100. Cassette P_1–D_3 encodes the signal sequence and mature protein up to residue 255, and so on. The shuttle plasmids containing the various cassettes were named as derivatives of pRD100. For example, that containing P_1–D_3 is referred to as pRD100(1–3). As before, note that all plasmids direct the production of fusion proteins with 39 vector-derived amino acids preceding the amino terminus of the cloned peptide itself.

Shuttle plasmids containing each of the 16 truncated cassettes were introduced into yeast, and the transformants so obtained were evaluated for growth characteristics on uracil-deficient galactose plates and for production of immunoreactive Slt-IA product. Lethality of the cloned toxin for the host was preserved in plasmids carrying cassettes P_1–D_3, P_2–D_4, and P_2–D_3 but in no others (Table I). In other words, the shortest toxic fragment defined began at the mature start site, ended at residue 255, and was virtually identical to the A_1 fragment of ST described by Olsnes et al. (1981). N-Terminal truncations distal to the mature start site or C-terminal truncations proximal to the presumed A_1 fragment cleavage site were not toxic. All toxic clones and several of the shorter, nontoxic ones (P_2–D_2, P_3–D_3, and P_3–D_4) made immuno-

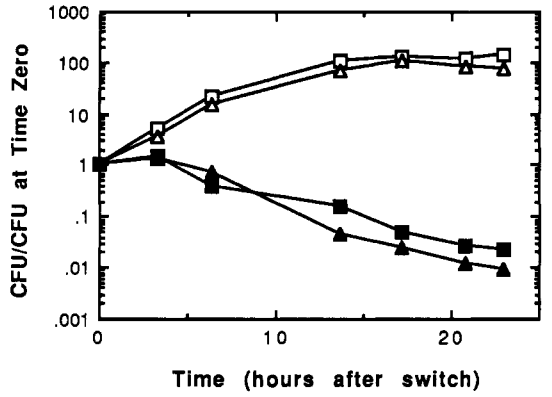

FIGURE 6: Growth in various sugars of yeast cells bearing pRD100 or pRD100(1–3). At T_0, early log-phase cultures that had been growing in glucose broth were harvested, washed, and split to either glucose or galactose broth. Incubation was resumed. Data points reflect the number of colony-forming units per milliliter in each culture at time T divided by the number in that same culture at time T_0. pRD100/glucose (□), pRD100/galactose (■), pRD100(1–3)/glucose (△), pRD100(1–3)/galactose (▲).

reactive products of the expected size.

The yeast strain containing deletion plasmid pRD100(1–3) was also evaluated for growth characteristics in liquid medium. As shown in Figure 6, induction of the cloned element was associated with a fall in colony-forming units per milliliter qualitatively and quantitatively similar to that occurring with induction of the full-length clone, pRD100.

Molecular Modeling. The coordinates on which the model of Slt-IA is based are those of the A chain of the ricin heterodimer. Figure 7 (top) shows the superposition of the α-carbon traces of the known crystallographic structure of RTA and of the computer model of Slt-IA. Certain residues of Slt-IA are labeled, and the α-carbons of five putative active-site residues are shown as spheres. The amino terminus of Slt-IA is marked by the number 1. That of RTA is eight residues longer and is unmarked. The carboxy terminus of Slt-IA is 36 residues longer than that of RTA. Since Slt-IA residues 258–293 have no analogues in RTA, a reasonable model for that portion of the molecule could not be made. Consequently residue 257, which is matched with RTA residue 267, marks the C terminus of the model of Slt-IA. Five putative active-site residues (Tyr 77, Tyr 114, Glu 167, Arg 170, and Trp 203 in Slt-IA), shown as spheres in the top panel of Figure 7, are shown in greater detail in the bottom panel.

DISCUSSION

As predicted from the known action of Slt-IA on eukaryotic ribosomes, expression of Slt-IA in *S. cerevisiae* is lethal to the host. That lethality was exploited to select a spontaneous point mutant of *slt*-IA that had lost the ability to kill yeast yet still produced full-length immunoreactive Slt-IA protein. Because that selection was independent of any prior conceptual model of the structure of the toxin's active site, it permitted an unbiased approach to the problem of identifying active-site residues. Indeed, although tyrosine 77 was known to be conserved among members of the ricin toxin family (Ready et al., 1988), its importance as a residue potentially in the active site was revealed by the current study.

The frequency of stable attenuated point mutants of Slt-IA arising in our system (one of about 250 surviving clones) was lower than that reported by Frankel and colleagues in the ricin system (12 of 72 surviving clones) (Frankel et al., 1989). This difference might be due to any of several factors, chief among

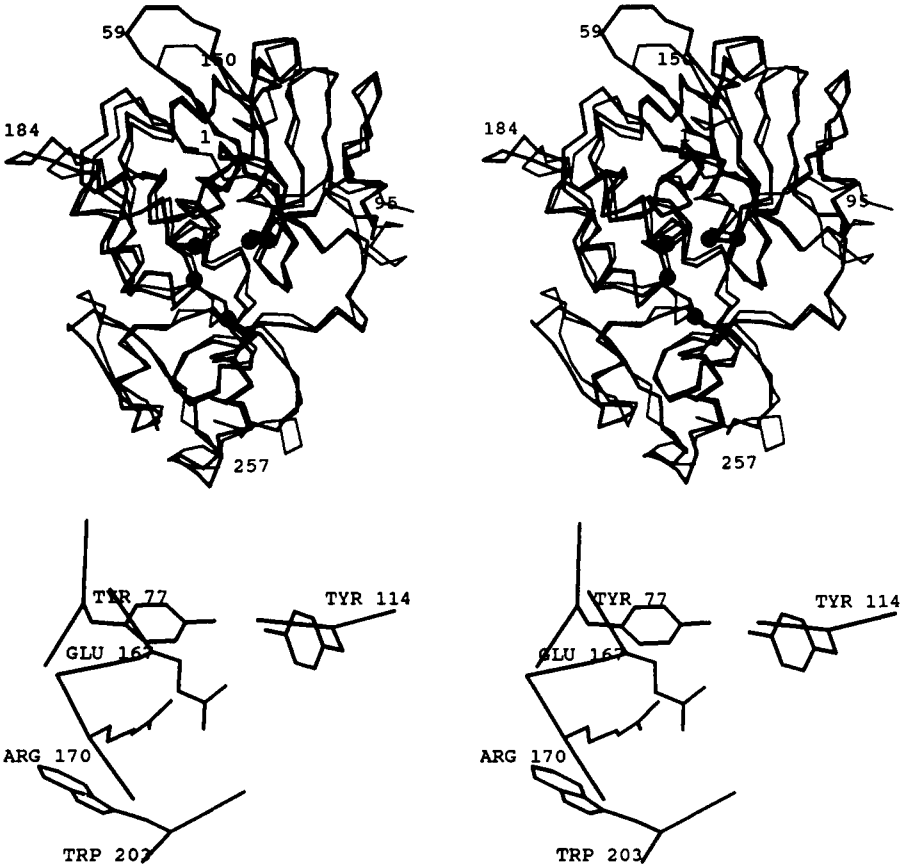

FIGURE 7: (Top) Superposition of the molecular models of Slt-IA and RTA. The α-carbon backbone of Slt-IA has darker bonds; the numbers refer to this model. Five active-site residues are shown as spheres. (Bottom) Active site of Slt-IA. This divergent stereopair looks from the model into the solvent and shows the geometric relationship of five key residues implicated in the mechanism of action.

them that Frankel's group performed biological mutagenesis on their ricin expression plasmid prior to introducing it into the yeast cells, while we relied on the random appearance of attenuating point mutants once our Slt-IA expression plasmid had already been inserted into the host cells. Of course, intrinsic differences in the two proteins or in the host strains might contribute to this discrepancy as well. In order to verify that mutants attenuated in the ability to inhibit protein synthesis in vitro are indeed also attenuated in their ability to kill yeast (and thus to test the veracity of our selection system), we created a yeast expression plasmid bearing the mutation Slt-IA (E167D). As expected, that construct was devoid of evident toxicity to the yeast host but still produced full-length, immunoreactive Slt-IA product. There is good evidence, therefore, that selection of surviving yeast clones, as described, is a valid means to generate attenuated mutants of Slt-IA. We did not perform saturation mutagenesis nor did we perform an exhaustive search for CRM-positive clones. Had we done so, it is likely that we would have isolated additional species of interest.

We have shown by two separate means that the mutation Y77S drastically reduces activity of Slt-IA. Yeast cells bearing the plasmic pRD100(Y77S) were able to grow on galactose with the same growth kinetics as those containing the nontoxic control plasmid pRY131. pRD100 producing wild-type Slt-IA rapidly killed the yeast cells under similar conditions. Moreover, that same mutation diminished by at least 1000-fold the ability of Slt-IA in periplasmic extract of *E. coli* to inhibit protein synthesis by rabbit reticulocyte lysates.

The more conservative mutation Y77F was also measurably attenuated in both assay systems: though yeast cells carrying pRD100(Y77F) were not able to increase in viable cell density when grown on galactose, neither were they killed by the mutant Slt-IA. The in vitro correlate of that nonlethal growth arrest was an attenuation by 10–20-fold of the ability of the corresponding protein in periplasmic extract to inhibit peptide synthesis by reticulocyte lysate. This finding is consistent with the independently made observation that the corresponding change Y80F in RTA reduced activity 15-fold (Ready et al., 1991).

As in all active-site mutagenesis studies, our data is limited by the difficulty of proving that the attenuating effects of the Y77 mutations are indeed due to modification of a critical active-site component rather than to global alteration in protein folding. While we have not fully ruled out the possibility that major conformational changes are responsible for the diminished activity of the mutant proteins, two lines of reasoning suggest otherwise. The mutation Y77F is highly conservative, differing from the wild type only by the absence of a phenolic hydroxy group. It is unlikely that such a small change would cause major structural perturbations. As well, the pattern and degree of breakdown of the mutant toxins Y77S and Y77F was essentially identical to that of wild-type Slt-IA, as assessed by Western blots. There was no evidence that either mutant was destabilized. It is therefore reasonable to conclude that tyrosine 77 may play an important role in enzymatic function.

In ricin, three aromatic residues have been identified in the putative active-site cleft: Tyr 80, Tyr 123, and Trp 211, homologous to Slt-IA Tyr 77, Tyr 114, and Trp 203, respectively. The attenuating effect of the RTA mutation Y80F has already been mentioned. Similarly, the mutation Y123F decreased the activity 7-fold (Ready et al., 1991), while the mutation W211F decreased the activity 9-fold (Bradley & McGuire, 1990). In the molecular model of Slt-IA, the three homologous aromatics all cluster in the vicinity of a candidate

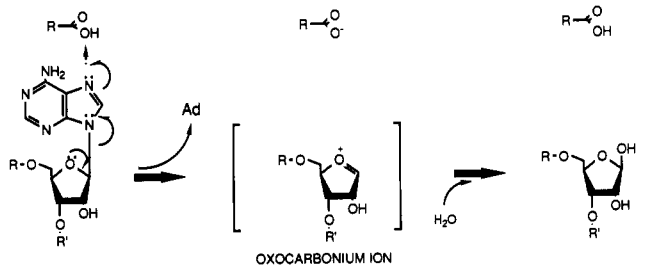

FIGURE 8: Putative S_N1 mechanism for RNA N-glycosidase action. An acid catalyst protonates the target adenine at one of the ring nitrogens. This action sets up an electron sink that destabilizes the carbon–nitrogen bond between the 1′ ribose carbon and the number 9 adenine nitrogen. The adenine leaves. The resultant oxocarbonium ion is attacked by water, a weak nucleophile, which adds a hydroxyl group to the ribose ring and restores the acid catalyst.

active-site pocket (Figure 7, bottom). The phenolic rings of Tyr 77 and Tyr 114 line the top wall of the pocket, while the heterocyclic rings of Trp 203 form a portion of the bottom wall. At the base of the pocket lie Glu 167 and Arg 170. Significantly, all five residues are invariant in the ricin toxin family.

In addition to looking for attenuating point mutations, we used deletion analysis to define smaller domains of Slt-IA that retain enzymatic activity. Any such domain identified must by definition contain the active-site machinery in an appropriate conformation. The PCR primers that were used to define the deletion cassettes studied here were chosen without regard to specific models of the Slt-IA active site. The shortest truncated fragment that retained activity was P_2–D_3, the cassette corresponding almost exactly to the A_1 fragment previously prepared by proteolysis of whole ST-A and previously shown to be toxic. Inspection of the computer model of Slt-IA, which itself corresponds almost exactly to the A_1 fragment, shows that the next shortest C-terminal deletion (cassette P_2–D_2; residues 1–187) is lacking many of the residues that form the left wall of the proposed active site. By the same token, the next shortest N-terminal deletion (cassette P_3–D_3; residues 65–255) is deleted of all but the 12 residues immediately N-terminal to tyrosine 77. Surely in that cassette tyrosine 77 is displaced from its normal position. Thus, in retrospect, it is perfectly consistent with the model presented here that all the truncated mutants shorter than P_2–D_3 that we studied were inactive. Indeed, one would expect them to be inactive.

In considering the chemistry of an RNA N-glycosidase, one might imagine that catalysis proceeds via an S_N1 mechanism (Figure 8): an acid catalyst protonates the target adenine moiety at one of the ring nitrogens and thereby destabilizes the carbon–nitrogen bond between the 1′ ribose carbon and the number 9 adenine nitrogen. The protonated adenine dissociates from the ribose backbone, leaving behind a positively charged oxocarbonium ion intermediate that is stabilized by negative charges in the immediate environment. A water molecule attacks the positive charge, hydroxylates the ribose ring, and restores the acid catalyst, thereby completing the process. The same mechanism has been independently proposed for the action of the ricin A chain (Ready et al., 1991).

Features that ought to be present in the active site of such an enzyme include chemical species to promote docking and to orient the target ribosomal adenine nucleotide, an acid catalyst to promote leaving by that adenine, and negatively charged species to stabilize the putative oxocarbonium ion intermediate. One model by which the above-described active-site geometry might meet these requirements posits the following tentative functional assignments: Arg 170 might form an ion pair with the ribose–phosphate backbone and

thereby help tether the toxin to its RNA substrate; the aromatics might, through a stacking interaction, stabilize and position the target adenine; and Glu 167 might stabilize the positively-charged intermediate. It is possible that the acid catalyst is not supplied by a discrete, strongly acidic species as such but rather by the additive effects of several weakly acidic groups. In particular, the weakly acidic phenolic hydroxyl of Tyr 77 might participate in this way. A similar scheme has been proposed for the mechanism of RTA, based in part on the work of Schramm and colleagues (Ready et al., 1991). It accounts nicely for the moderate functional impact of the mutation Y77F and the major impact of Y77S.

As further enzymatic and crystallographic information becomes available, it should be possible to focus or reject the details of this preliminary model. Until then, we hope that it will provide a useful framework for workers in this field.

ACKNOWLEDGMENTS

We thank Arthur Frankel for helpful advice regarding the yeast expression system and for the plasmid pRY131, Art Donohue-Rolfe for donating Shiga toxin and antiserum to Shiga toxin, Fred Winston for the gift of yeast strain Fy2, and Larry Mattheakis, Sims Kochi, and Brenda Wislon for many helpful discussions.

REFERENCES

Bradley, J. L., & McGuire, P. M. (1990) *Int. J. Pept. Protein Res. 35*, 365–366.

Brunger, A. T., Kuriyan, J., & Karplus, M. (1987) *Science 235*, 458–460.

Calderwood, S. B., Auclair, F., Donohue-Rolfe, A., Keusch, G. T., & Mekalanos, J. J. (1987) *Proc. Natl. Acad. Sci. U.S.A. 84*, 4364–4368.

Collins, E. J., Robertus, J. D., LoPresti, M., Stone, K. L., Williams, K. R., Wu, P., Hwang, K., & Piatak, M. (1990) *J. Biol. Chem. 265*, 8665–8669.

Dickie, N., Speirs, J. I., Akhtar, M., Johnson, W., & Szabo, R. A. (1989) *J. Clin. Microbiol. 27*, 1973–1978.

Endo, Y., & Tsurugi, K. (1987) *J. Biol. Chem. 262*, 8128–8130.

Endo, Y., Mitsui, K., Motizuki, M., & Tsurugi, K. (1987) *J. Biol. Chem. 262*, 5908–5912.

Endo, Y., Tsurugi, K., Yutsudo, T., Takeda, Y., Ogasawara, T., & Igarashi, K. (1988) *Eur. J. Biochem. 171*, 45–50.

Frankel, A., Schlossman, D., Welsh, P., Hertler, A., Withers, D., & Johnson, S. (1989) *Mol. Cell. Biol. 9*, 415–420.

Frankel, A., Welsh, P., Richardson, J., & Robertus, J. D. (1990) *Mol. Cell. Biol. 10*, 6257–6263.

Griffin, P. M., Ostroff, S. M., Tauxe, R. V., Greene, K. D., Wells, J. G., Lewis, J. H., & Blake, P. A. (1988) *Ann. Intern. Med. 109*, 705–712.

Hoffman, C. S., & Winston, F. (1987) *Gene 57*, 267–272.

Hovde, C. J., Calderwood, S. B., Mekalanos, J. J., & Collier, R. J. (1988) *Proc. Natl. Acad. Sci. U.S.A. 85*, 2568–2572.

Jackson, M. P., Deresiewicz, R. L., & Calderwood, S. B. (1990) *J. Bacteriol. 72*, 3346–3350.

Jones, T. A. (1978) *J. Appl. Crystallogr. 11*, 268–272.

Karmali, M. A., Petric, M., Lim, C., Fleming, P. C., Abrus, G. S., & Lior, H. (1985) *J. Infect. Dis. 151*, 775–782.

Katzin, B. J., Collins, E. J., & Robertus, J. D. (1991) *Proteins: Struct., Funct., Genet. 10*, 251–259.

Maniatis, T., Fritsch, E. F., and Sambrook, J. (1982) *Molecular Cloning: A Laboratory Manual*, Cold Spring Harbor Laboratory, Cold Spring Harbor, NY.

Montfort, W., Villafranca, J. E., Monzingo, A. F., Ernst, S. R., Katzin, B., Rutenber, E., Xuong, N. H., Hamlin, R., & Robertus, J. D. (1987) *J. Biol. Chem. 262*, 5398–5403.

O'Brien, A. D., & Holmes, R. K. (1987) *Microbiol. Rev. 51*, 206–220.

Olsnes, S., Reisbig, R., & Eiklid, K. (1981) *J. Biol. Chem. 256*, 8732–8738.

Ready, M. P., Katzin, B. J., & Robertus, J. D. (1988) *Proteins: Struct., Funct., Genet. 3*, 53–59.

Ready, M. P., Kim, Y., & Robertus, J. D. (1991) *Proteins: Struct., Funct., Genet. 10*, 270–278.

Reisbig, R., Olsnes, S., & Eiklid, K. (1981) *J. Biol. Chem. 256*, 8739–8744.

Schlossman, D., Withers, D., Welsh, P., Alexander, A., Robertus, J., and Frankel, A. (1989) *Mol. Cell. Biol. 9*, 5012–5021.